The phosphorylation status of Ser-637 in dynamin-related protein 1 (Drp1) does not determine Drp1 recruitment to mitochondria

Received for publication, February 26, 2019, and in revised form, September 12, 2019 Published, Papers in Press, September 18, 2019, DOI 10.1074/jbc.RA119.008202

Rong Yu[‡1], **Tong Liu**[‡1], **Chenfei Ning**[‡], **Fei Tan**[‡], **Shao-Bo Jin**[§], **Urban Lendahl**[§], **Jian Zhao**[‡2,3], **and Monica Nistér**[‡2,4]

From the [‡]*Department of Oncology-Pathology, Karolinska Institutet, Karolinska University Hospital Solna, Stockholm, Sweden and* [§]*Department of Cell and Molecular Biology, Karolinska Institutet, Stockholm, Sweden*

Edited by John M. Denu

Recruitment of the GTPase dynamin-related protein 1 (Drp1) to mitochondria is a central step required for mitochondrial fission. Reversible Drp1 phosphorylation has been implicated in the regulation of this process, but whether Drp1 phosphorylation at Ser-637 determines its subcellular localization and fission activity remains to be fully elucidated. Here, using HEK 293T cells and immunofluorescence, immunoblotting, RNAi, subcellular fractionation, co-immunoprecipitation assays, and CRISPR/Cas9 genome editing, we show that Drp1 phosphorylated at Ser-637 (Drp1^{pS637}) resides both in the cytosol and on mitochondria. We found that the receptors mitochondrial fission factor (Mff) and mitochondrial elongation factor 1/2 (MIEF1/2) interact with and recruit Drp1^{pS637} to mitochondria and that elevated Mff or MIEF levels promote Drp1^{pS637} accumulation on mitochondria. We also noted that protein kinase A (PKA), which mediates phosphorylation of Drp1 on Ser-637, is partially present on mitochondria and interacts with both MIEFs and Mff. PKA knockdown did not affect the Drp1-Mff interaction, but slightly enhanced the interaction between Drp1 and MIEFs. In Drp1-deficient HEK 293T cells, both phosphomimetic Drp1-S637D and phospho-deficient Drp1-S637A variants, like wild-type Drp1, located to the cytosol and to mitochondria and rescued a Drp1 deficiency-induced mitochondrial hyperfusion phenotype. However, Drp1-S637D was less efficient than Drp1-WT and Drp1-S637A in inducing mitochondrial fission. In conclusion, the Ser-637 phosphorylation status in Drp1 is not a determinant that controls Drp1 recruitment to mitochondria.

Mitochondrial morphology is highly dynamic, controlled by a balance between mitochondrial fission and fusion (collectively termed mitochondrial dynamics) (1, 2). In mammalian cells, mitochondria are organized into dynamic tubular networks that frequently change their morphology and cellular distribution via fission and fusion events in response to metabolic demands or pathological conditions (2–6). Aberrant regulation of the mitochondrial fission/fusion balance causes mitochondrial dysfunction and has been implicated in human disease (7–16).

In mammals, the mitochondrial fusion machinery consists of three key dynamin-related GTPases: the two outer membrane–anchored GTPases, mitofusin 1 and 2 (Mfn1 and Mfn2), and the inner membrane–anchored GTPase OPA1. Mfn1 and Mfn2 are highly homologous and anchored in the outer mitochondrial membrane by two transmembrane segments (17). Mfn1 and Mfn2 on adjacent mitochondria can form homodimers and heterodimers through *trans*-interactions, tethering the outer membranes of adjacent mitochondria together (18). Therefore, Mfn1 and Mfn2 are essential for fusion of mitochondrial outer membranes, whereas OPA1 is critical for fusion of the inner membranes (7, 19).

The dynamin-related GTPase Drp1 is a core component of the mitochondrial fission machinery and plays a central role in mitochondrial fission. Drp1 is primarily distributed in the cytosol of mammalian cells, but shuttles between the cytosol and the mitochondrial surface (20, 21), and translocation of Drp1 to mitochondria has emerged as a key step in mitochondrial fission. In mammals, Drp1 is recruited from the cytosol to the mitochondrial surface via its receptors Mff,[5] MIEFs (MIEF1 and MIEF2, also known as MiD51 and MiD49) and Fis1 (22–30). At the mitochondrial surface Drp1 is assembled into higher-order complexes (oligomers) at endoplasmic reticulum–mitochondrial contact sites and wrap around the mitochondria to induce mitochondrial fission via its GTPase activity (31–35). Therefore, Drp1-mediated mitochondrial fission is believed to be a multi-step process requiring the sequential and coordinated interaction of Drp1 with a number of other fission-promoting factors. For instance, endoplasmic reticulum, together with actin-filaments, plays a crucial role in establishing constriction sites before Drp1 recruitment (36, 37) and Dyn2 coordinates with Drp1 at the final step of mitochondrial division (38).

This work was supported by the Swedish Research Council (VR-NT, VR-MH, and VR-Linné), Swedish Cancer Society, ICMC (AstraZeneca), BRECT Consortium at Karolinska Institutet, Cancer Society in Stockholm and Karolinska Institutet Grants. This work was also supported by the Knut and Alice Wallenberg Foundation (CLICK facility). The authors declare that they have no conflicts of interest with the contents of this article.

This article contains Figs. S1 and S2.

[1] These authors contributed equally to this work.

[2] These authors share senior responsibility.

[3] To whom correspondence may be addressed: BioClinicum, J5:30, Karolinska University Hospital Solna, Stockholm, Sweden. E-mail: jian.zhao@ki.se.

[4] To whom correspondence may be addressed: BioClinicum, J5:30, Karolinska University Hospital Solna, Stockholm, Sweden. E-mail: monica.nister@ki.se.

[5] The abbreviations used are: Mff, mitochondrial fission factor; MIEF, mitochondrial elongation factor; PCC, Pearson's correlation coefficient; pAb, polyclonal antibody; co-IP, co-immunoprecipitation

The fission activity of Drp1 can be modulated by multiple posttranslational modifications, such as ubiquitylation, SUMOylation, *S*-nitrosylation, and phosphorylation (39–42). Phosphorylation of Drp1 is the most studied posttranslational modification regulating mitochondrial fission, and phosphorylation occurs at two serine residues: Ser-616 and Ser-637 (in human Drp1 isoform 1) (33, 39, 40). Drp1–Ser-616 phosphorylation is cell cycle–regulated via Cdk1/cyclin B and causes mitochondrial fragmentation (43). Drp1–Ser-637 is phosphorylated by the cAMP-dependent protein kinase A (PKA), which likely inhibits mitochondrial fission through impairing Drp1 GTPase activity and preventing translocation of Drp1 to mitochondria (44–46). Conversely, dephosphorylation at Ser-637 by calcineurin appears to increase mitochondrial recruitment of Drp1, in turn promoting mitochondrial fission (45, 46). Reversible phosphorylation of Drp1 may play a critical role in regulating its subcellular localization and fission activity, but many aspects of Drp1 phosphorylation are still not fully understood. For instance, whether the phosphorylation status of Drp1 in fact determines its subcellular localization and/or direct interaction with mitochondrial receptors MIEFs and Mff remains to be elucidated.

In this study, we address the role of Drp1 phosphorylation at Ser-637 (Drp1^{pS637}) for subcellular localization and ability to regulate mitochondrial fission. We show that Drp1^{pS637} distributes to both the cytosol and mitochondria and does not play a major role in controlling mitochondrial fission.

Results

Phosphorylated Drp1^{S637} is present on mitochondria

The phosphorylation status of Drp1–Ser-637 has been proposed to influence recruitment of Drp1 to mitochondria as well as its efficiency in mitochondrial fission (33, 39, 40, 42). To address this issue, we first examined the level of phosphorylated Drp1–Ser-637 (Drp1^{pS637}) in 293T cells and found that the basal level was very low in these cells, but could be rapidly elevated by treatment with the PKA activator forskolin, and even further by a combination of forskolin with the calcineurin inhibitor FK506 (Fig. 1*A*, *lanes 1*, *2*, and *4*). In contrast, no elevation was observed with FK506 alone (Fig. 1*A*, *lane 3*), whereas phospho-Drp1–Ser-616 (Drp1^{pS616}) was easily detected in 293T cells by Western blotting in all these cases (Fig. 1*A*). The specificity of the antibodies used for detecting total Drp1, Drp1^{pS637}, and Drp1^{pS616} is shown in Fig. S1.

To analyze the subcellular distribution of Drp1^{pS637}, we therefore used a combination of forskolin and FK506 treatment to enhance expression levels of Drp1^{pS637} in cells followed by immunofluorescence confocal microscopy. As shown in Fig. 1, *B* and *C*, treatment with forskolin/FK506 greatly enhanced the amount of Drp1^{pS637} in 293T cells, and Drp1^{pS637} was present both at the mitochondrial surface and in the cytosol. Confocal microscopy combined with 3D surface rendering revealed that Drp1^{pS637} localized to the pre- and post-fission sites and overlapped with total Drp1 on the surface of mitochondria (Fig. 1, *D* and *E*, *arrows*). Quantitative co-localization analysis using Pearson's correlation coefficient (PCC) confirmed that the increased amount of Drp1^{pS637} was accompanied by an increased co-localization of Drp1^{pS637} with mitochondria (Fig. 1*F*). These results indicated that Drp1^{pS637} can be recruited to the mitochondrial surface and/or that Drp1 can be phosphorylated when localized on mitochondria.

Additionally, we found that forskolin treatment increased the percentage of cells with tubular mitochondria (Fig. 1*G*), in keeping with previous observations (44–46). This appears to be consistent with the view that phosphorylation of Drp1 at Ser-637 inhibits Drp1-mediated fission, leading to mitochondrial elongation. However, we found that a further increase in the level of Drp1^{pS637} by forskolin/FK506 treatment resulted in the opposite effect on mitochondrial morphology, *i.e.* a promotion of mitochondrial fragmentation (Fig. 1*G*). These results imply that the phosphorylation status of Drp1 at S637 does not play a crucial role in forskolin- or forskolin/FK506-induced alterations of mitochondrial dynamics, and that additional mechanisms are involved in regulating mitochondrial morphology.

MIEFs and Mff recruit Drp1^{pS637} as well as nonphospho-Drp1^{S637} to the surface of mitochondria

It was reported previously that Mff and MIEFs (MIEF1 and MIEF2) interact with and recruit Drp1 from the cytosol to mitochondria (23–27) but whether Drp1^{pS637} is recruited in a similar manner was not addressed. We therefore examined effects of overexpression of Mff, MIEF1, or MIEF2 on the subcellular localization of total Drp1 and Drp1^{pS637} after treatment with forskolin plus FK506 by confocal microscopy. Consistent with previous studies (23–27), overexpression of Myc-Mff, MIEF1-V5, or MIEF2-V5 enhanced levels of total Drp1 on mitochondria (Fig. 2*A*, *middle panels*). Meanwhile, we found that overexpression of Myc-Mff, MIEF1-V5, or MIEF2-V5 also increased the accumulation of Drp1^{pS637} on mitochondria in 293T cells treated with forskolin plus FK506 compared with empty vector control cells (Fig. 2*A*, *lower panels*). Consistent with this, Drp1/mitochondria co-localization analysis by PCC showed a significant increase of Drp1^{pS637} on mitochondria in cells transfected with Mff, MIEF1, or MIEF2 compared with control (empty vector) (Fig. 2*B*). In agreement with these results, subcellular fractionation analysis revealed that Drp1^{pS637} was present both on mitochondria and in the cytosol of 293T cells treated with forskolin plus FK506 (Fig. 2, *C* and *D*). Overexpression of either Mff or MIEFs also resulted in a relatively increased amount of Drp1^{pS637} and total Drp1 in the mitochondrial fractions (Fig. 2, *C* and *D*). Collectively, these data indicate that Drp1^{pS637} is recruited to mitochondria by Mff and MIEFs.

MIEFs and Mff interact with Drp1^{pS637} and nonphospho-Drp1^{S637}

We next assessed whether Mff and MIEFs interact with Drp1^{pS637}. Overexpression of either MIEFs or Mff in 293T cells did not significantly affect levels of total Drp1 and phosphorylated Drp1–Ser-616 (Drp1^{pS616}) in cells (Fig. 3*A*, *Input*), and co-immunoprecipitation revealed that Drp1^{pS616} interacted with the two MIEFs as well as with Mff, but the binding to Mff was relatively lower than to MIEF1 and MIEF2 in normal cells (Fig. 3*A*, *IP*). As the endogenous levels of Drp1^{pS637} in the absence of PKA stimulation were too low for conclusions to be

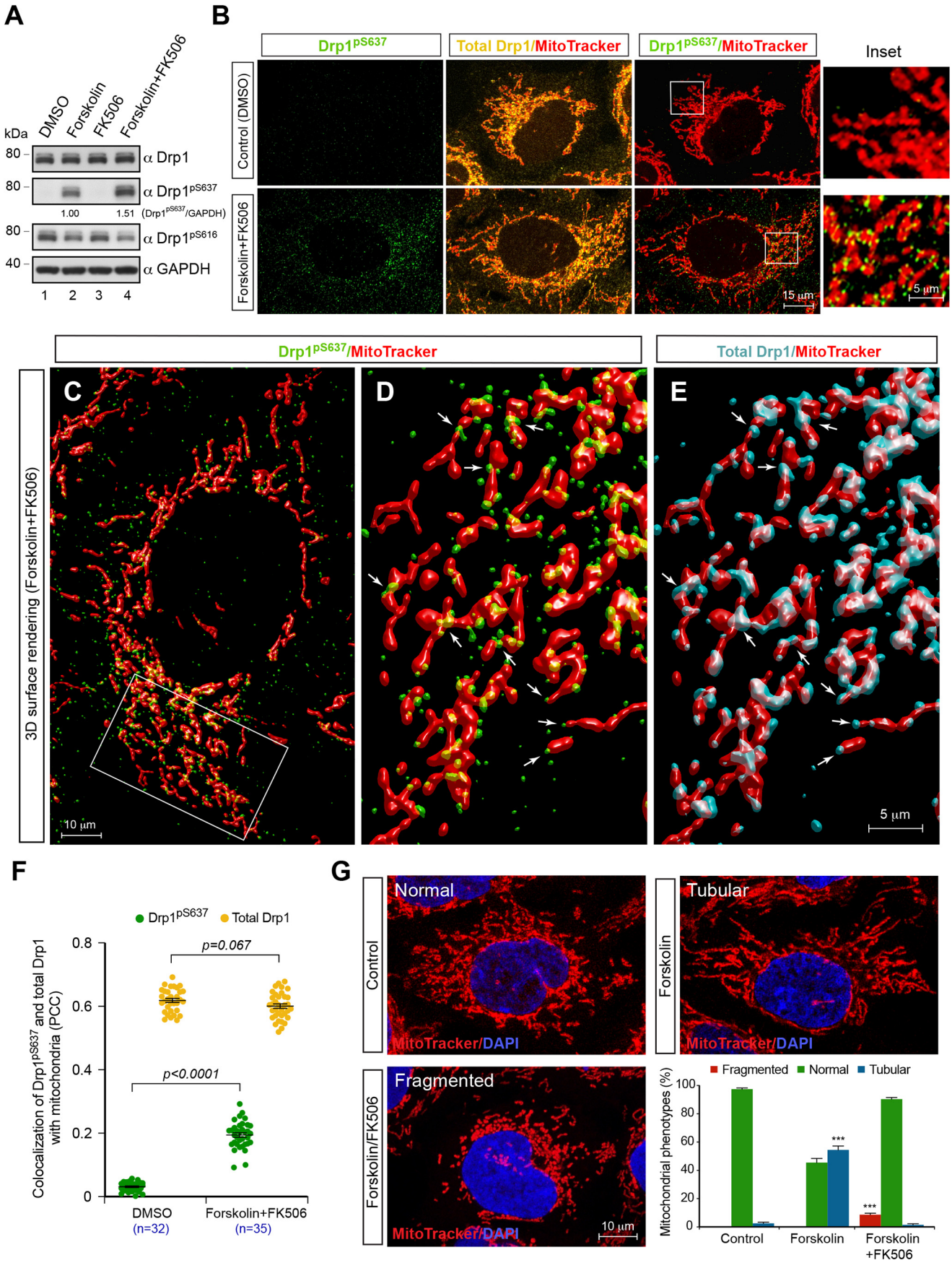
A
DMSO
Forskolin
FK506
Forskolin+FK506
kDa
80
α Drp1
80
α Drp1pS637
1.00
1.51
(Drp1pS637/GAPDH)
80
α Drp1pS616
40
α GAPDH
1 2 3 4
B
Drp1pS637
Total Drp1/MitoTracker
Drp1pS637/MitoTracker
Inset
Control (DMSO)
Forskolin+FK506
15 μm
5 μm
Drp1pS637/MitoTracker
Total Drp1/MitoTracker
3D surface rendering (Forskolin+FK506)
C
D
E
10 μm
5 μm
F
Drp1pS637
Total Drp1
p=0.067
p<0.0001
Colocalization of Drp1pS637 and total Drp1 with mitochondria (PCC)
0.8
0.6
0.4
0.2
0
DMSO
(n=32)
Forskolin+FK506
(n=35)
G
Control
Normal
MitoTracker/DAPI
Forskolin
Tubular
MitoTracker/DAPI
Forskolin/FK506
Fragmented
MitoTracker/DAPI
10 μm
Fragmented
Normal
Tubular
Mitochondrial phenotypes (%)
100
80
60
40
20
0
***
***
Control
Forskolin
Forskolin +FK506

drawn (Fig. 3*A*), we performed MIEFs and Mff co-IP experiments following forskolin treatment. The data reveal that Drp1^{pS637} interacted with both MIEFs and Mff (Fig. 3*B*), with a relatively higher proportion of Drp1^{pS637} relative to total Drp1 in the Mff-Drp1 complex than in the MIEF1-Drp1 and MIEF2-Drp1 complexes (Fig. 3*D*). A similar result was obtained when cells were treated with another PKA activator, 8-bromo-cAMP (Fig. 3, *C* and *D*). However, the proportion of Drp1^{pS637} relative to total Drp1 in the Mff-Drp1 complex was slightly different for the forskolin *versus* the 8-bromo-cAMP treated cells (Fig. 3, *B–D*). Co-immunoprecipitation with a Drp1^{pS637}-specific antibody after forskolin treatment confirmed that Drp1^{pS637} interacted with both MIEFs and Mff at endogenous levels (Fig. 3*E*).

We recently reported that MIEFs serve as a molecular bridge linking Drp1 and Mff in a trimeric Drp1-MIEF-Mff complex on mitochondria and facilitate a direct physical binding of Drp1 to Mff via a transition of Drp1 from a trimeric Drp1-MIEF-Mff complex to a dimeric Drp1-Mff complex (30). These findings prompted us to explore whether ablation of endogenous MIEFs could also affect the binding of Drp1^{pS637} to Mff. First, co-IP experiments revealed that the enhanced cellular levels of Drp1^{pS637} induced by forskolin treatment did not affect the interaction of endogenous Mff with total Drp1 (Fig. 3*F*). However, knockdown of both MIEF1/2 by siRNA greatly reduced the amount of Drp1^{pS637} as well as the amount of total Drp1 bound to Mff (Fig. 3*G*), indicating that endogenous MIEFs promoted the association of Mff with both Drp1^{pS637} and non-phospho-Drp1^{S637}. Collectively, these data lead us to conclude that MIEFs and Mff may interact with and recruit Drp1^{pS637} to mitochondria.

PKA is not a major factor for regulating the interaction of Drp1 with Mff and MIEFs

Because PKA is a major kinase that phosphorylates Drp1 at Ser-637 (44, 45, 47), we explored potential roles of PKA in regulating Drp1 subcellular localization and the association of Drp1 with MIEFs and Mff. First, we showed that PKA was present in both the mitochondrial and the cytosolic fractions in 293T cells (Fig. 4*A*), and PKA partially appeared as punctate structures on mitochondria (Fig. 4*B*) in line with a previous report (47). Co-IP experiments revealed that endogenous PKA interacted with exogenously expressed MIEFs and Mff, but the interaction of PKA with Mff was much weaker than with MIEFs (Fig. 4*C*). Furthermore, knockdown of Drp1 by siRNA resulted in an increased interaction between MIEFs and PKA (Fig. 4*D*), implying that PKA bound to MIEFs independently of Drp1. We next evaluated potential effects of PKA knockdown on the association of Drp1 with Mff and MIEFs. Depletion of PKA by siRNA slightly increased the interaction of Drp1 with MIEF1 and MIEF2 (Fig. 4*E*) but had no discernable effect on the interaction between total Drp1 and Mff at endogenous levels (Fig. 4*F*). These results indicate that PKA is not a major factor in regulating the interaction of Drp1 with Mff and MIEFs.

The phosphorylation status of Drp1 mildly affects mitochondrial fission but is not a determinant controlling the recruitment of Drp1 to mitochondria

Drp1, in mammalian cells, is thought to exist as multiple assembly units including dimers, tetramers, and higher-order oligomers in a dynamic equilibrium (48–51). Therefore, to exclude potential interference of endogenous WT Drp1 in these experiments as well as interference of the tag linked to Drp1, we used a Drp1-deficient (Drp1$^{-/-}$) 293T cell line generated by CRISPR/Cas9-mediated genome editing (52) and evaluated the effects of reconstituted untagged phosphomimetic (Drp1^{S637D}) and phospho-deficient (Drp1^{S637A}) versions on the subcellular distribution and function of Drp1 in these cells. In reconstituted Drp1$^{-/-}$ cells, the subcellular distribution of Drp1^{S637D} and Drp1^{S637A} was comparable to that of Drp1 (Drp1^{WT}) (Fig. 5*A*). Like Drp1^{WT}, Drp1^{S637D} and Drp1^{S637A} mutants were distributed both in the cytosol and on mitochondria. Quantitative Drp1/mitochondrial co-localization analysis by PCC further confirmed that neither of the mutants had a significantly altered distribution on mitochondria (Fig. 5*B*). Moreover, Drp1^{S637D} and Drp1^{S637A} both efficiently reversed the mitochondrial hyperfusion phenotype caused by loss of endogenous Drp1 (Fig. 5*A*). However, Drp1^{S637D} expression resulted in a small but statistically significant decrease in the number of cells with fragmented mitochondria, whereas Drp1^{S637A} expression led to a slight increase (but did not reach statistical significance) compared with Drp1^{WT}. These data indicate that Drp1^{S637D} is less efficient in mitochondrial fission compared with Drp1^{WT} and Drp1^{S637A} (Fig. 5*C*). No difference in subcellular distribution was observed in Drp1$^{-/-}$ cells expressing Drp1^{S616A} and Drp1^{S616D}, compared with Drp1^{WT} (Fig. 5, *A* and *B*). In contrast to Drp1^{S637D}, the phosphomimetic Drp1^{S616D} was more efficient than Drp1^{S616A} and Drp1^{WT} in inducing mitochondrial fragmentation (Fig. 5*C*), consistent with a previous study (53).

We next assessed the effects of forskolin/FK506 treatment on phosphorylation of Drp1^{WT}, Drp1^{S637D}, and Drp1^{S637A} in Drp1$^{-/-}$ cells. Forskolin/FK506 treatment only induced phos-

Figure 1. Drp1^{pS637} is present in the cytosol but also on mitochondria. *A*, the basal level of phosphorylated Drp1^{pS637} is very low in 293T cells but can be boosted by treatments either with the PKA activator forskolin or with forskolin plus FK506 (a calcineurin inhibitor), but not with FK506 alone. 293T cells were treated with DMSO (control), forskolin (30 μM), FK506 (10 μM), or forskolin (30 μM) plus FK506 (10 μM) for 3 h. Cell lysate was subjected to immunoblotting with indicated antibodies. The ratio of Drp1^{pS637}/GAPDH was analyzed by densitometry. GAPDH was used as loading control. *B*, confocal images showing subcellular localization of Drp1^{pS637} and total Drp1 after forskolin/FK506 treatment. 293T cells treated with DMSO (control) or with forskolin (30 μM) plus FK506 (10 μM) for 3 h and stained with MitoTracker (*red*), anti–phospho-Drp1 (Ser-637) (*green*), and anti-Drp1 antibody (*yellow*, for detecting total Drp1). *Insets* represent high magnification views of the *boxed areas*. *C*, 3D surface rendering reconstruction of the cell treated with forskolin plus FK506 as shown in the *lower panel* in *B*. The Drp1^{pS637} (*green*) and total Drp1 (*cyan*) proteins, as well as mitochondria (*red*) are indicated. *D* and *E*, the high magnification views of the *boxed area* in (*C*) show overlaps of Drp1^{pS637} (*green*) with total Drp1 (*cyan*) at pre- and post-fission sites on mitochondria (*arrows*). *F*, quantitative co-localization of Drp1^{pS637} and total Drp1 with mitochondria (from *B*) was analyzed using the PCC (mean ± S.E.M.) in cells treated with DMSO or forskolin plus FK506. *n* represents the number of cells analyzed. *G*, forskolin treatment induces mitochondrial elongation, but forskolin plus FK506 treatment induces mitochondrial fragmentation. Confocal images of mitochondrial morphology in 293T cells treated with DMSO (control), forskolin (30 μM), or forskolin (30 μM) plus FK506 (10 μM) for 3 h prior to harvest. Percentages (mean ± S.E.M.) of cells with indicated mitochondrial morphologies in 293T cells treated with DMSO ($n = 249$), forskolin ($n = 262$), or forskolin plus FK506 ($n = 500$), respectively. *n* represents the number of cells analyzed. ***, $p < 0.0001$.

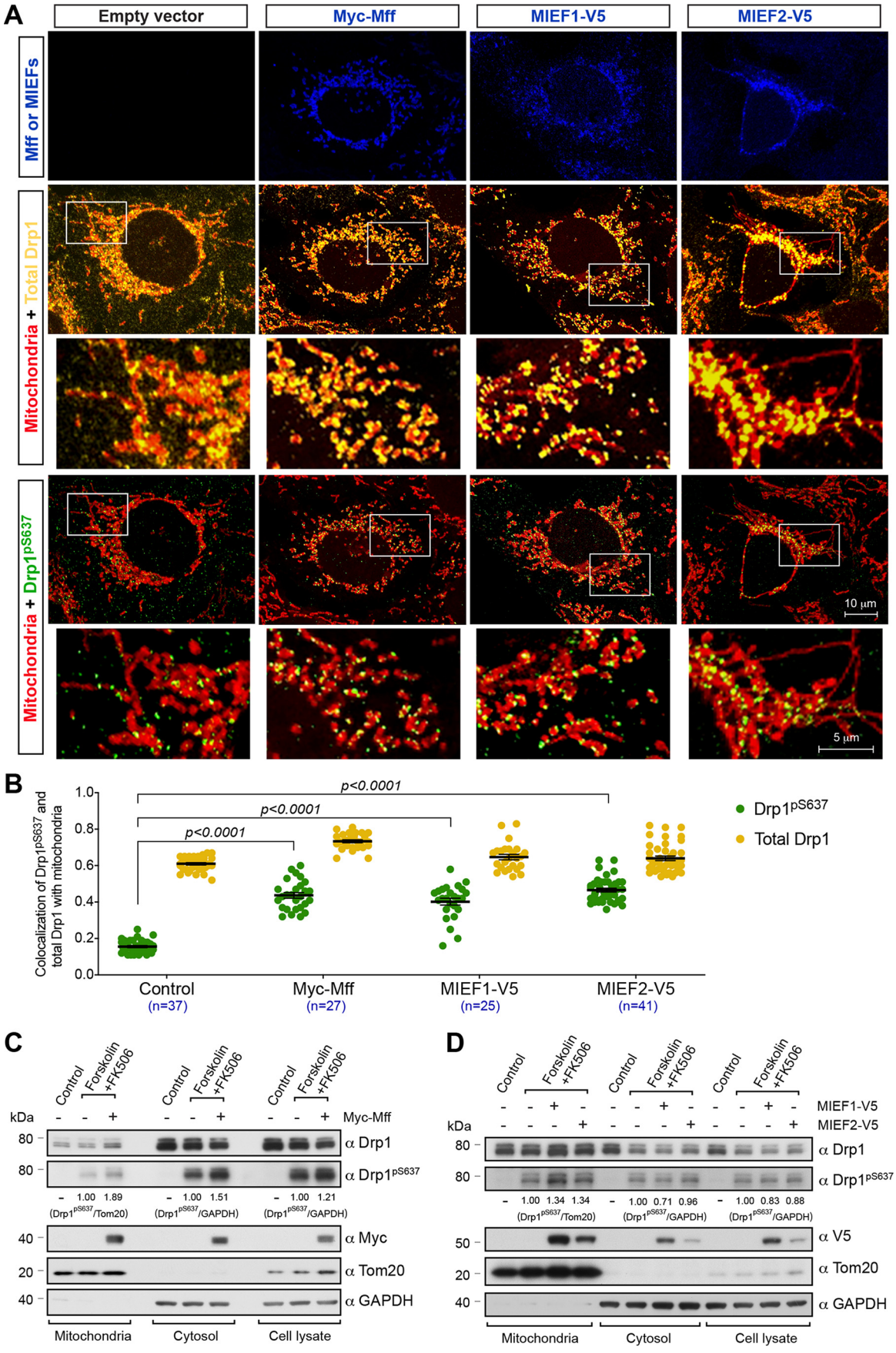
A
Empty vector
Myc-Mff
MIEF1-V5
MIEF2-V5
Mff or MIEFs
Mitochondria + Total Drp1
Mitochondria + Drp1pS637
10 μm
5 μm
B
Colocalization of Drp1pS637 and total Drp1 with mitochondria
p<0.0001
p<0.0001
p<0.0001
Drp1pS637
Total Drp1
Control (n=37)
Myc-Mff (n=27)
MIEF1-V5 (n=25)
MIEF2-V5 (n=41)
C
Control
Forskolin +FK506
kDa
Myc-Mff
α Drp1
α Drp1pS637
(Drp1pS637/Tom20)
(Drp1pS637/GAPDH)
α Myc
α Tom20
α GAPDH
Mitochondria
Cytosol
Cell lysate
D
MIEF1-V5
MIEF2-V5
α V5

phorylation of Drp1^{WT} at Ser-637, but not of the mutants Drp1^{S637D} and Drp1^{S637A}, as observed by immunofluorescence microscopy (Fig. 6, *A–D*) and further confirmed by Western blot analysis (Fig. 6*E*; see also Fig. S2). Like total Drp1, phosphorylated Drp1 (Drp1^{pS637}) was distributed in the cytosol and on mitochondria in Drp1$^{-/-}$ cells expressing Drp1^{WT} (Fig. 6, *A–C*). These data further support the notion that Drp1 phosphorylated at Ser-637 does not prevent the translocation of Drp1 to mitochondria. Similarly, we found that Drp1^{S637D} was still less efficient in mitochondrial fragmentation compared with Drp1^{WT} and Drp1^{S637A} following forskolin/FK506 treatment (Fig. 6*D*), in line with the results without forskolin/FK506 treatment in Fig. 5*C*.

To explore potential mechanisms by which Drp1^{S637A} and Drp1^{S637D} differentially affect mitochondrial fission, we evaluated the interaction of Mff and MIEFs with untagged Drp1^{WT}, Drp1^{S637D}, and Drp1^{S637A} in Drp1$^{-/-}$ cells. Co-IP with anti-Mff antibody revealed that endogenous Mff interacted with Drp1^{WT} and the two mutants, but the phosphomimetic Drp1^{S637D} mutant exhibited a relatively weak interaction, whereas Drp1^{S637A} showed a strong interaction with Mff, compared with WT Drp1 (Fig. 7*A*). No obvious differences were observed in the interaction between MIEFs and Drp1^{WT}, Drp1^{S637A}, or Drp1^{S637D} (Fig. 7*B*). Furthermore, we evaluated the interaction of the phosphomimetic Drp1^{S637D} and the phospho-deficient Drp1^{S637A} mutants with MIEFs and Mff in WT 293T cells. Likewise, we found that Myc-Drp1^{S637D} showed a diminished, whereas the phospho-deficient Myc-Drp1^{S637A} exhibited an enhanced interaction with FLAG-Mff (Fig. 7*C*), in line with a recent study (54). No clear difference was observed for the interactions of MIEF1/2 with WT Drp1, Drp1^{S637A} and Drp1^{S637D} (Fig. 7*C*). Given that Mff serves as the major mitochondrial receptor to promote Drp1-mediated fission as reported previously (22, 23, 55), a decreased interaction between Drp1^{S637D} and Mff may thus explain why Drp1^{S637D} is less efficient in inducing mitochondrial fragmentation, in line with the results in Fig. 5*C*.

In sum, the data presented here indicate that the phosphorylation status of Drp1 at Ser-637 does not play a pivotal role in determining whether Drp1 is recruited to mitochondria through Mff and MIEFs. However, the phosphomimetic Drp1^{S637D} mutation slightly impairs, whereas the phosphomimetic Drp1^{S616D} in contrast, enhances mitochondrial fragmentation.

The phosphorylation status of Drp1 is not crucial for regulating Drp1-mediated peroxisomal fission

Drp1 is also involved in peroxisomal fission and maintenance of peroxisomal morphology in mammalian cells (56). However, whether the phosphorylation status at Drp1–Ser-637 affects peroxisomal fission remains to be determined (57), and we therefore analyzed the effect of Drp1 mutation at Ser-637 on the appearance of peroxisomes. In WT 293T cells, peroxisomes appeared as numerous small, punctiform organelles. However, depletion of Drp1 caused peroxisomal elongation and resulted in a tubular network of peroxisomes, similar to the mitochondrial network in Drp1-deficient cells (Fig. 8*A*), in line with previous reports (56, 58). Reconstituting Drp1$^{-/-}$ cells with untagged Drp1^{WT} rescued the peroxisomal fission defect induced by loss of Drp1 and reversed the appearance of elongated peroxisomes to a punctiform phenotype (Fig. 8, *B*, *C*, and *F*), which was comparable to that seen in WT cells (Fig. 8*A*). Similarly, re-introduction of untagged Drp1^{S637A} or Drp1^{S637D} into Drp1$^{-/-}$ cells resulted in a WT punctiform appearance of peroxisomes in a majority of cells (Fig. 8, *D* and *E*). The fragmented peroxisomal phenotype mediated by Drp1^{S637A} or Drp1^{S637D} was indistinguishable from that of Drp1^{WT} (Fig. 8*C*). In conclusion, these data suggest that the Drp1 Ser-637 phosphorylation status does not play a crucial role in regulating the activity of Drp1-mediated peroxisomal fission.

Discussion

Drp1 is recruited to mitochondria to execute mitochondrial fission, but the role of phosphorylation at Ser-637 in these processes has not been firmly established. Several studies have suggested that Drp1 phosphorylation at residue Ser-637 by PKA inhibits mitochondrial fission by decreasing the intramolecular interactions that normally drive GTPase activity and by preventing translocation of Drp1 to mitochondria, whereas dephosphorylation at Ser-637 increases mitochondrial recruitment of Drp1 and promotes mitochondrial fission (44–46, 54). However, it was not established in those studies whether the phosphorylation status at Drp1–Ser-637 is a determinant directly controlling the mitochondrial recruitment of Drp1. It has also been suggested that the phosphomimetic Drp1^{S637D} mutant is almost completely cytosolic and inhibits mitochondrial fission, whereas the phospho-deficient Drp1^{S637A} mutant shows enhanced translocation of Drp1 to mitochondria, promoting fission (44–46, 54).

In this study, we provide evidence that Drp1 phosphorylated at Ser-637 is present both on mitochondria and in the cytosol of 293T cells, and when cellular levels of Drp1^{pS637} are enhanced, the amount of Drp1^{pS637} on mitochondria correspondingly increases. Moreover, we show that Drp1^{pS637} interacts with MIEFs and Mff, and in line with this, overexpression of either Mff or MIEFs leads to accumulation of Drp1^{pS637} on mitochondria as seen by co-localization studies and confirmed by subcellular fractionation. Increasing the cellular levels of Drp1^{pS637} by PKA activation using forskolin does not prevent the recruitment of Drp1 to mitochondria. In addition, we show that PKA

Figure 2. Overexpression of Mff or MIEFs induces accumulation of Drp1^{pS637} on mitochondria. *A*, subcellular localization of Drp1^{pS637} and total Drp1 in 293T cells overexpressing Myc-Mff, MIEF1-V5, or MIEF2-V5. Confocal images of Drp1^{pS637} in 293T cells transfected with empty vector, Myc-Mff, MIEF1-V5, and MIEF2-V5, followed by treatment with forskolin (30 μM) plus FK506 (10 μM) for 3 h, and staining with MitoTracker (*red*), anti–phospho-Drp1 (Ser-637) (*green*), anti-Drp1(*yellow*), and either anti-Myc (*blue*) or anti-V5 antibodies (*blue*) as indicated. The high magnification views of the *boxed areas* as indicated. *B*, quantitative co-localization of Drp1^{pS637} and total Drp1 with mitochondria (from *A*) was analyzed using the PCC (mean ± S.E.M.). *n* represents the number of cells analyzed. *C* and *D*, subcellular fractionation of 293T cells, treated with DMSO (control) or forskolin (30 μM) plus FK506 (10 μM) for 3 h, and transfected with Myc-Mff (*C*) or with either MIEF1-V5 or MIEF2-V5 (*D*), followed by immunoblotting analysis with indicated antibodies. The ratio between indicated proteins was analyzed by densitometry in the mitochondrial and cytosolic fractions as well as in whole cell lysate. Tom20 was used for loading control of the mitochondrial fraction and GAPDH for the cytosolic fraction. The ratio between indicated proteins was analyzed by densitometry.

is present not only in the cytosol but also on mitochondria, where it interacts with MIEF1 and MIEF2, as well as Mff. In agreement with this, the mitochondria-anchored scaffold protein AKAP1 (protein kinase A anchoring protein 1) is known to recruit PKA to the mitochondrial surface, and in turn mitochondria-associated PKA phosphorylates Drp1–Ser-637 (47, 59). We show here that PKA is not a major regulator of the interaction of Drp1 with Mff and MIEFs. It should, however, be kept in mind that PKA is a multifunctional kinase with a broad range of substrates. PKA can induce phosphorylation of numerous proteins localized on the mitochondrial outer membrane and within mitochondria (60–62). Thus, PKA-depen-

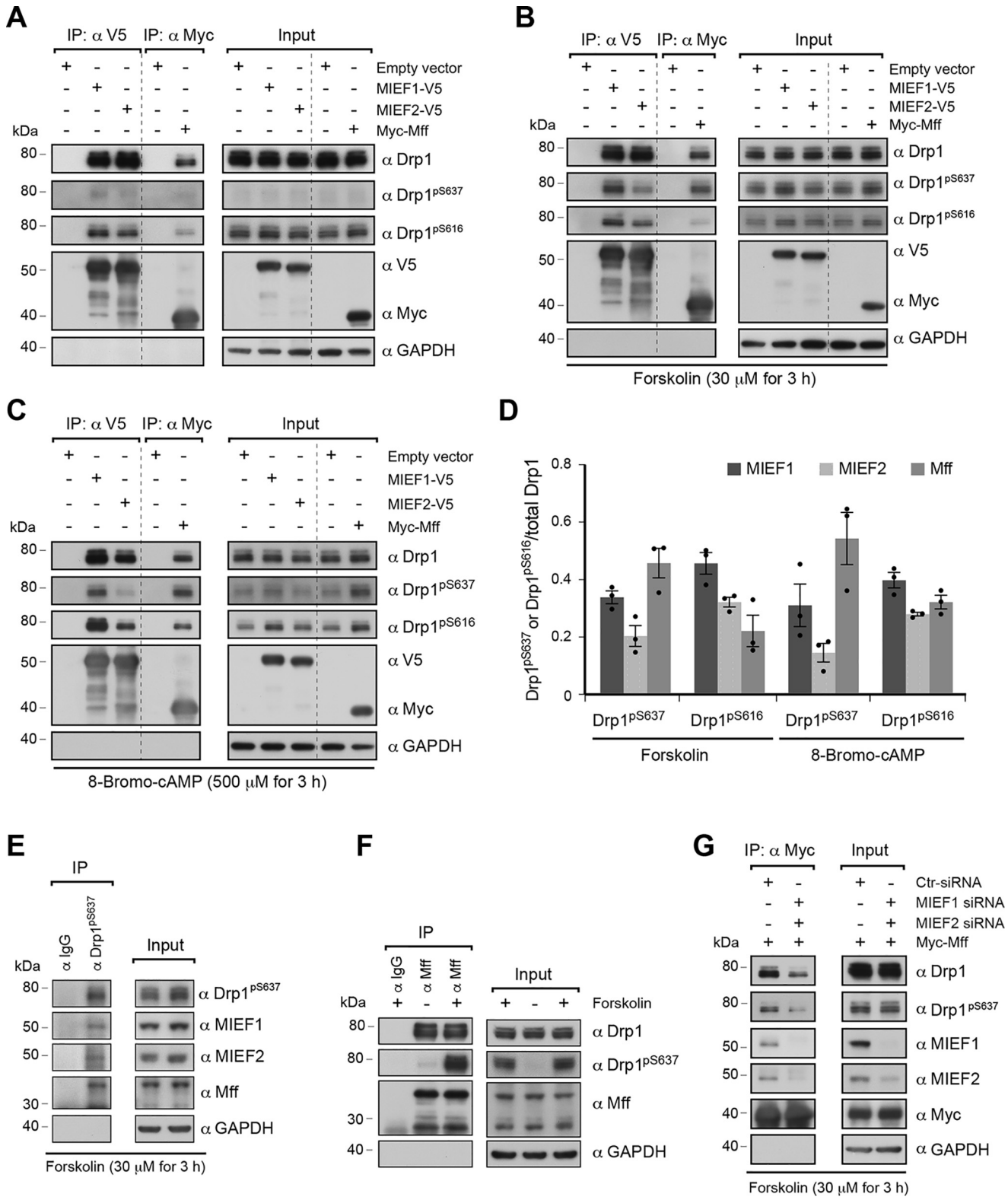

dent phosphorylation is not only directly involved in regulating mitochondrial dynamics, but also affects a number of other biological processes in mitochondria, such as mitochondrial protein import, oxidative phosphorylation, fatty acid oxidation, mitochondrial Ca^{2+} homeostasis, mitophagy, and apoptosis (33, 61, 63, 64). PKA-mediated changes of these biological processes are also likely to influence mitochondrial dynamics (14, 33, 65–67). Moreover, it cannot be excluded that PKA may phosphorylate other mitochondria-shaping proteins; it was for instance reported that Mfn2 can be phosphorylated by PKA (68). Here we showed that PKA interacts with the MIEF1, MIEF2, and Mff, although the potential roles of the interactions between PKA and MIEFs or Mff remain to be elucidated. In sum, these data indicate that PKA may influence mitochondrial dynamics in multiple ways and alterations in mitochondrial morphology should not be regarded simply as a functional consequence of the Drp1–Ser-637 phosphorylation. Reconstitution of Drp1 expression in $Drp1^{-/-}$ cells showed that both $Drp1^{S637D}$ and $Drp1^{S637A}$ mutants, like WT Drp1, were similarly distributed in the cytosol and on mitochondria. Collectively, these data are at odds with the view that Drp1 phosphorylated at amino acid Ser-637 ($Drp1^{pS637}$) by PKA is retained in the cytosol (46, 54), and instead support the notion that $Drp1^{pS637}$ still can shuttle between the cytosol and mitochondria. We thus conclude that phosphorylation at Ser-637 does not prevent Drp1 translocation to mitochondria and that the Drp1–Ser-637 phosphorylation status is not a determinant controlling the recruitment of Drp1 to mitochondria (via Mff and MIEFs).

However, the reversible phosphorylation at Drp1–Ser-637 may play a minor role in regulating mitochondrial recruitment and fission activity of Drp1 via differential association with the Mff and MIEF receptors. As shown in our co-IP experiments, $Drp1^{pS637}$ likely differentially interacted with Mff, MIEF1, and MIEF2. When analyzing the Drp1–Ser-637 mutants, co-IP showed that the association of Mff with the phosphomimetic $Drp1^{S637D}$ was attenuated compared with $Drp1^{WT}$ and $Drp1^{S637A}$, in line with the results presented in a recent report (54), but our findings do not support the view that dephosphorylation at Drp1–Ser-637 is essential for Drp1's interaction with Mff and MIEFs. Moreover, the phosphomimetic $Drp1^{S637D}$ was recruited to mitochondria as efficiently as $Drp1^{WT}$ and $Drp1^{S637A}$ when introduced into $Drp1^{-/-}$ cells, although the phosphomimetic $Drp1^{S637D}$ was less efficient in inducing mitochondrial fragmentation than $Drp1^{WT}$ and $Drp1^{S637A}$. Taken together, we suggest that Drp1 phosphorylation at Ser-637 may slightly weaken but not abolish the Drp1-mediated mitochondrial fission activity. Consistent with this scenario, a previous study showed that Drp1 GTPase activity is only attenuated but not abolished by phosphorylation of Drp1 at Ser-637 or by $Drp1^{S637D}$ mutant (44). In contrast to $Drp1^{S637D}$, reconstitution of Drp1 expression in $Drp1^{-/-}$ cells showed that phosphomimetic $Drp1^{S616D}$ appears to be more active than $Drp1^{WT}$ and $Drp1^{S616A}$ in fragmenting mitochondria, in line with a recent report (53). The data support the view that phosphorylation of Drp1–Ser-616 enhances mitochondrial fission as reported previously (69).

In conclusion, this work shows that the phosphorylation status of Drp1 at Ser-637 is not a determinant primarily controlling its recruitment from the cytosol to mitochondria. Still it may fine-tune the differential association of Drp1 with mitochondrial membrane receptors (adaptors) and function to balance Drp1-mediated fission activity.

Experimental procedures

Cell cultures and transfection

HEK 293T cells (293T) and CRISPR/Cas9-edited Drp1 knockout 293T cells ($Drp1^{-/-}$) (52) were cultured in Dulbecco's modified Eagle's medium (HyClone) with 10% fetal bovine serum. Transient transfection with plasmids was performed using Lipofectamine® 2000 transfection reagent (Invitrogen) according to the manufacturer's protocol.

Antibodies and reagents

Mouse monoclonal antibodies (mAbs) used in this study were V5-tag (Invitrogen); Tom20, Drp1/DLP1 (611113), PKA, and Myc-tag (BD Biosciences); GAPDH (Santa Cruz Biotechnology); and PMP70 and FLAG-tag (Sigma). Rabbit polyclonal antibodies (pAbs) were V5-tag (Abcam); Mff (Atlas Antibodies); MIEF1 (24), MIEF2 and Myc-tag (Sigma); phospho-DRP1 (Ser-616) (rabbit pAb, 3455) and phospho-DRP1 (Ser-637) (D3A4, rabbit mAb, 6319) (Cell Signaling Technology). Goat polyclonal antibodies (pAbs) were Mff antibody (T-14) (Santa Cruz Biotechnology); V5-tag (Novus Biologicals); and Myc-tag (Abcam). Other antibodies included normal goat IgG and normal rabbit IgG (Santa Cruz Biotechnology). Secondary antibodies for immunofluorescence were The DyLight 488- and 649-conjugated anti-mouse and anti-rabbit IgG antibodies (Vector Laboratories) and Alexa Fluor 405 anti-goat IgG antibody (Abcam). For immunoblotting, the peroxidase-conjugated anti-mouse and anti-rabbit IgG antibodies (GE Healthcare) were used. Dynabeads® Protein G (Thermo Fisher Scientific) were used for co-IP experiments. Reagents used included forskolin, 8-bromo-cAMP, and FK506 (Tocris).

Figure 3. MIEFs and Mff interact with $Drp1^{pS637}$. *A* and *B*, MIEFs and Mff interact with $Drp1^{pS637}$. 293T cells were transfected with indicated plasmids, and then cells received no treatment (*A*) or were treated with the PKA activator forskolin (30 μM) for 3 h (*B*). Cell lysates were used for co-IP with anti-V5 or anti-Myc beads followed by immunoblotting with indicated antibodies. *C*, MIEFs and Mff interact with $Drp1^{pS637}$ in cells treated with the PKA activator 8-bromo-cAMP. 293T cells were transfected with empty vector, MIEF1-V5, MIEF2-V5, or Myc-Mff, and then treated with 8-bromo-cAMP (500 μM) for 3 h before harvest. Cell lysates were used for co-IP with anti-V5 or anti-Myc beads followed by immunoblotting analysis with indicated antibodies. *D*, the ratio (mean ± S.E.M.) between $Drp1^{pS637}$ or $Drp1^{pS616}$, and total Drp1in Mff, MIEF1, or MIEF2 complexes in (*B*) and (*C*) was analyzed by densitometry. The data are representative of three independent co-IP experiments. *E*, MIEFs and Mff interact with $Drp1^{pS637}$ at endogenous levels. 293T cells were treated with forskolin (30 μM) for 3 h. Cell lysates were used for co-IP with control (rabbit normal IgG) or rabbit anti–phospho-Drp1 (Ser-637) antibody and co-immunoprecipitated proteins were analyzed by immunoblotting with indicated antibodies. *F*, enhanced levels of $Drp1^{pS637}$ do not disrupt the association of endogenous Mff with total Drp1. 293T cells were treated with forskolin (30 μM) for 3 h as indicated. Cell lysates were used for co-IP with control (rabbit normal IgG) or rabbit anti-Mff antibody and co-immunoprecipitated proteins were analyzed by immunoblotting with indicated antibodies. *G*, knockdown of MIEF1/2 reduces the amount of total Drp1 and $Drp1^{pS637}$ bound to Mff. 293T cells were treated with control or MIEF1/2 siRNAs as indicated, and then transfected with Myc-Mff plasmid, followed by treatment with forskolin (30 μM) for 3 h. Cell lysates were used for co-IP with anti-Myc beads.

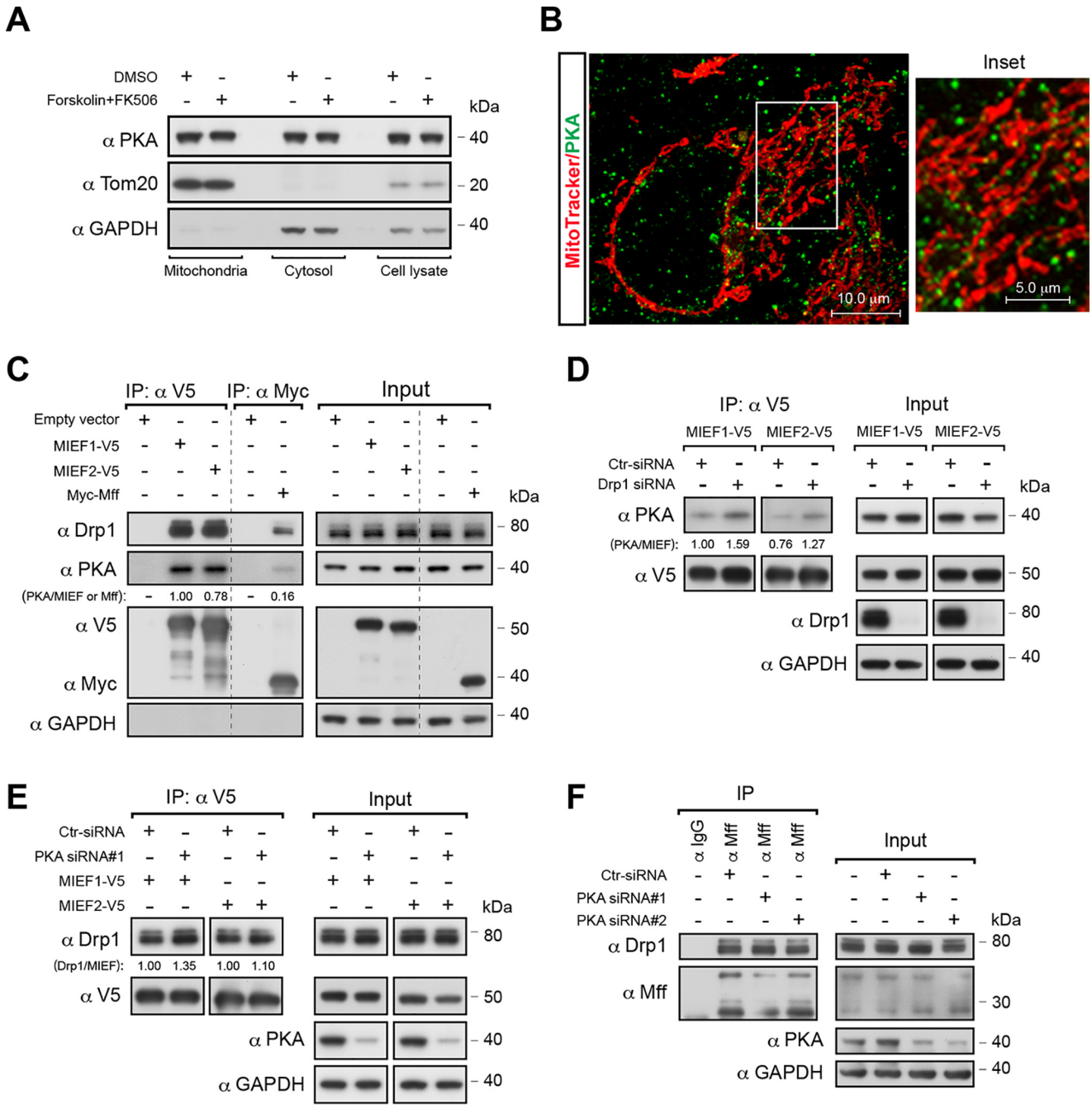

Figure 4. PKA interacts with MIEFs and Mff. *A*, subcellular distribution of PKA was analyzed by subcellular fractionation of 293T cells treated with and without forskolin plus FK506, followed by immunoblotting with indicated antibodies. *B*, endogenous PKA partially localizes on mitochondria. Immunofluorescence confocal image of normal 293T cells, stained with MitoTracker (*red*) and immunostained with anti-PKA antibody (*green*). *Inset* represents high magnification view of the *boxed area*. *C*, PKA is co-immunoprecipitated with MIEFs and Mff. 293T cells were transfected with indicated plasmids. Cell lysates were used for co-IP with anti-V5 or anti-Myc beads followed by immunoblotting with indicated antibodies. The ratio between indicated proteins was analyzed by densitometry. *D*, knockdown of Drp1 does not disrupt the association between MIEFs and PKA. 293T cells were treated with control or Drp1 siRNA, and then transfected with MIEF1-V5 or MIEF2-V5. Cell lysates were used for co-IP with anti-V5 beads, and immunoprecipitated proteins were subjected to immunoblotting with indicated antibodies. The ratio between indicated proteins was analyzed by densitometry. *E*, knockdown of PKA results in a slightly increased interaction between MIEFs and Drp1 in the absence of forskolin treatment. 293T cells were treated with control siRNA or PKA siRNA, and then transfected with MIEF1-V5 or MIEF2-V5 plasmids. Cell lysates were used for co-IP with anti-V5 beads followed by immunoblotting with indicated antibodies. The ratio between indicated proteins was analyzed by densitometry. *F*, knockdown of PKA does not affect the endogenous interaction between Mff and Drp1 in the absence of forskolin treatment. 293T cells were treated with control siRNA or different PKA siRNAs. Cell lysates were used for co-IP with control (rabbit normal IgG) or rabbit anti-Mff antibody and co-immunoprecipitated proteins were analyzed by immunoblotting with indicated antibodies.

Expression constructs used in this study included human MIEF1-V5 (24), MIEF2-V5 (26), Myc-Mff (human isoform 8) (28), FLAG-Mff (mouse isoform 8) (22), Myc-Drp1 (human isoform 1), Myc-Drp1^{S637A}, and Myc-Drp1^{S637D} (44). For generation of untagged WT Drp1, the cDNA was amplified by PCR using the Myc-Drp1 (human isoform 1) expression plasmid (44) as the template and cloned into the pcDNA3.1 vector (Invitrogen). The untagged Drp1^{S637A}, Drp1^{S637D}, Drp1^{S616A}

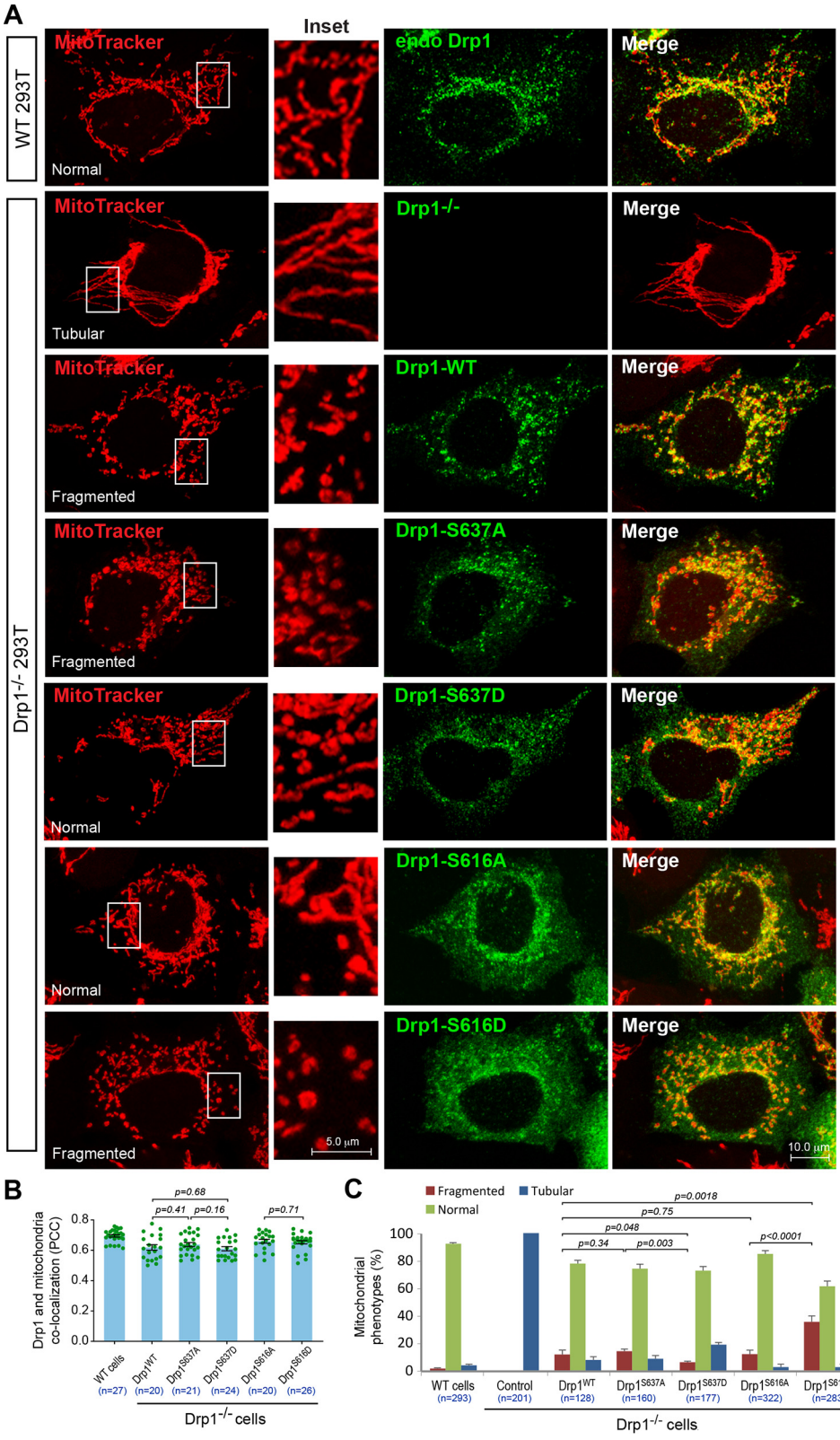

Figure 5. The Drp1 phosphorylation status is not crucial for controlling the mitochondrial recruitment of Drp1, but Drp1^{S637D} slightly impairs and Drp1^{S616D} mildly enhances Drp1-mediated fission. *A*, subcellular localization of Drp1 and morphology of mitochondria in WT and Drp1$^{-/-}$ 293T cells as well as in Drp1$^{-/-}$ 293T cells overexpressing untagged Drp1^{WT}, Drp1^{S637A}, Drp1^{S637D}, Drp1^{S616A}, and Drp1^{S616D}, and stained with MitoTracker (*red*) followed by immunostaining with anti-Drp1 antibody (*green*). *Insets* represent high magnification views of the *boxed areas*. *B*, quantitative co-localization of mitochondria with reconstituted untagged Drp1^{WT}, Drp1^{S637A}, Drp1^{S637D}, Drp1^{S616A}, and Drp1^{S616D} in Drp1$^{-/-}$ cells as shown in (*A*) was analyzed using the PCC (mean ± S.E.M.). *n* represents the number of cells analyzed. *C*, percentages (mean ± S.E.M.) of cells with indicated mitochondrial morphologies in WT 293T cells, Drp1$^{-/-}$ cells, and Drp1$^{-/-}$ cells reconstituted with untagged Drp1^{WT}, Drp1^{S637A}, Drp1^{S637D}, Drp1^{S616A}, or Drp1^{S616D}. *n* represents the number of cells analyzed.

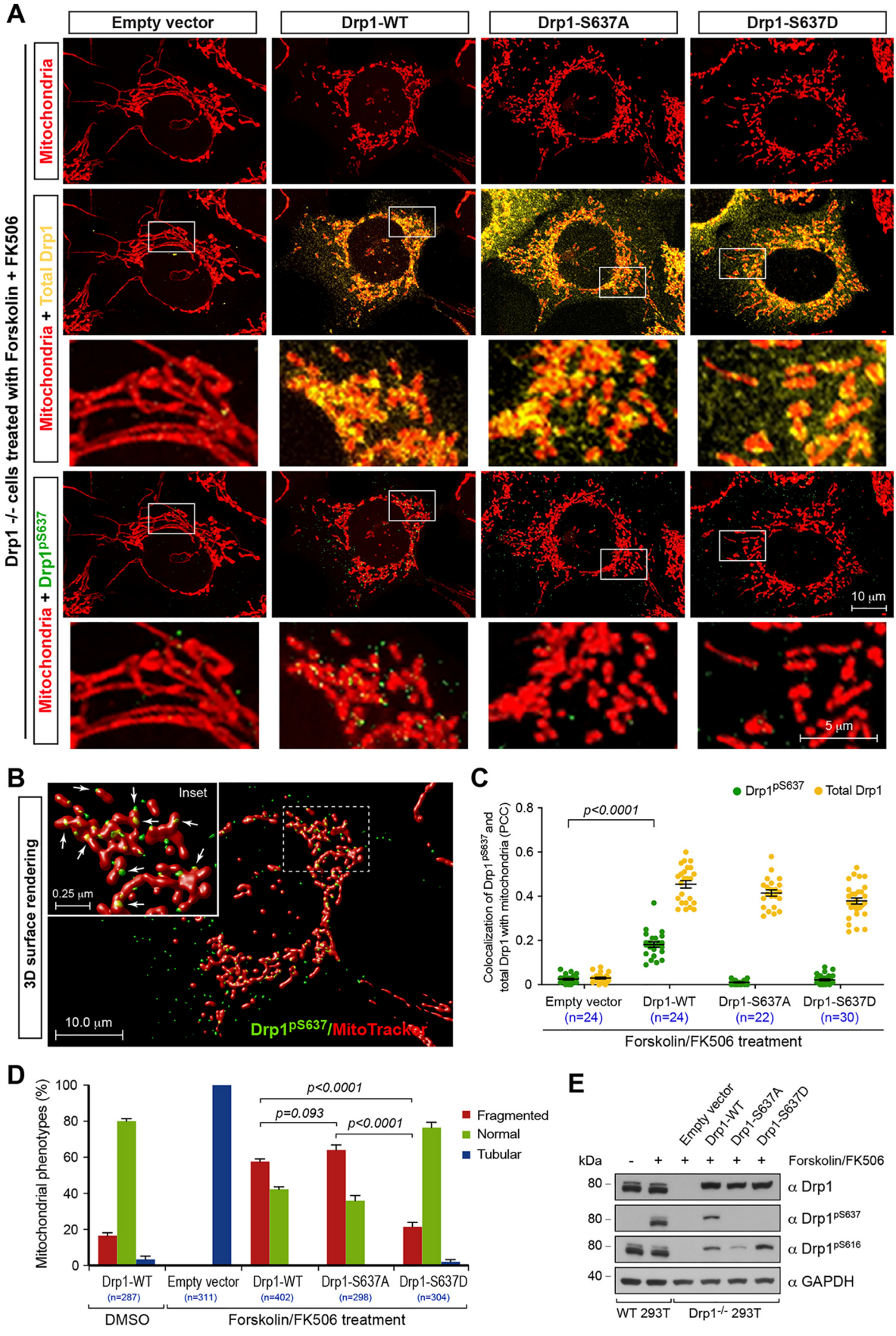
A
Empty vector
Drp1-WT
Drp1-S637A
Drp1-S637D
Mitochondria
Mitochondria + Total Drp1
Mitochondria + Drp1pS637
Drp1 -/- cells treated with Forskolin + FK506
10 μm
5 μm
B
3D surface rendering
Inset
0.25 μm
10.0 μm
Drp1pS637/MitoTracker
C
Drp1pS637
Total Drp1
p<0.0001
Colocalization of Drp1pS637 and total Drp1 with mitochondria (PCC)
0.8
0.6
0.4
0.2
0
Empty vector (n=24)
Drp1-WT (n=24)
Drp1-S637A (n=22)
Drp1-S637D (n=30)
Forskolin/FK506 treatment
D
Mitochondrial phenotypes (%)
100
80
60
40
20
0
p<0.0001
p=0.093
p<0.0001
Fragmented
Normal
Tubular
Drp1-WT (n=287)
Empty vector (n=311)
Drp1-WT (n=402)
Drp1-S637A (n=298)
Drp1-S637D (n=304)
DMSO
Forskolin/FK506 treatment
E
Empty vector
Drp1-WT
Drp1-S637A
Drp1-S637D
kDa
- + + + + +
Forskolin/FK506
80
α Drp1
80
α Drp1pS637
80
α Drp1pS616
40
α GAPDH
WT 293T
Drp1-/- 293T

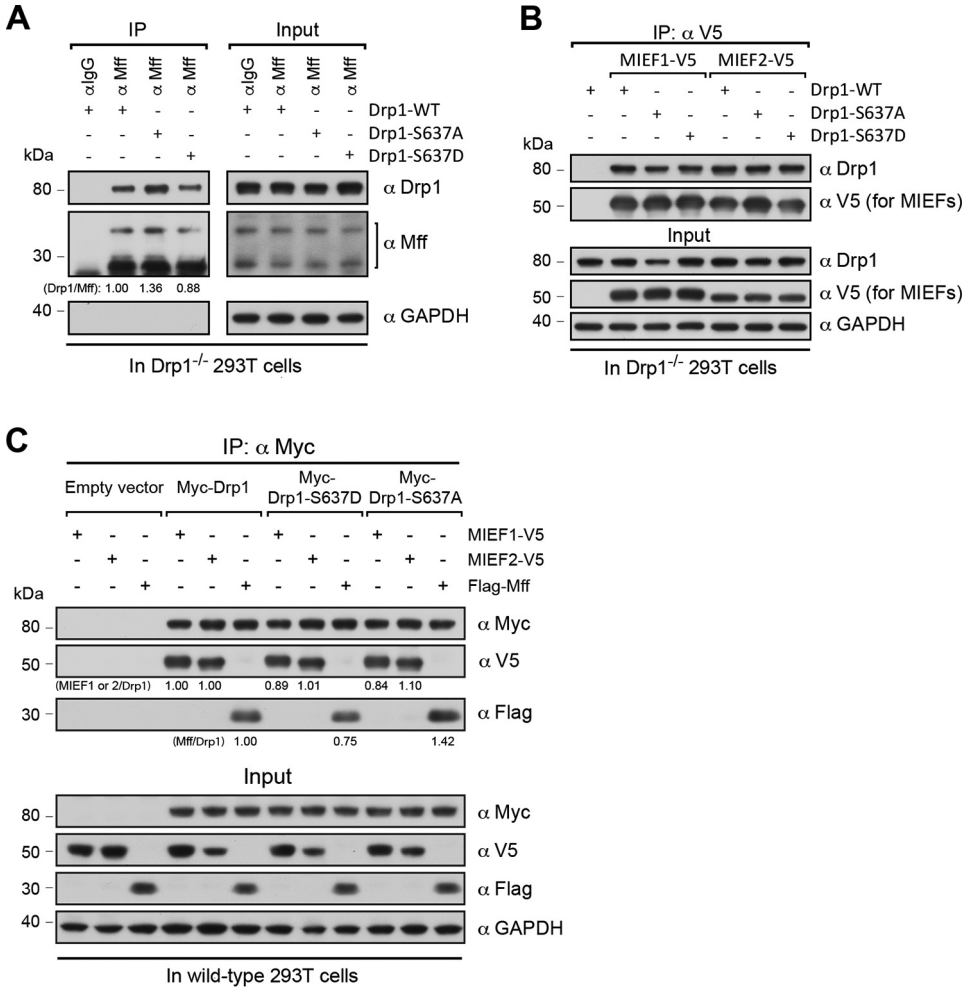

Figure 7. Mff and MIEFs interact with exogenous Drp1^{WT}, Drp1^{S637A}, and Drp1^{S637D} in the presence and absence of endogenous Drp1. *A* and *B*, Mff and MIEFs interact with WT Drp1, as well as with the phospho-deficient and phosphomimetic Drp1–Ser-637 mutants, Drp1^{S637A} and Drp1^{S637D} in Drp1-deficient 293T cells. Drp1$^{-/-}$ 293T cells were transfected with untagged Drp1^{WT}, Drp1^{S637A}, or Drp1^{S637D} only or co-transfected with MIEF1-V5 or MIEF2-V5 as indicated. Cell lysates were used for co-IP with anti-Mff antibody for endogenous Mff in (*A*) or anti-V5 antibody for exogenous MIEFs in (*B*) followed by immunoblotting with indicated antibodies. *C*, MIEFs and Mff interact with WT Drp1, as well as with the phospho-deficient and phosphomimetic Drp1–Ser-637 mutants, Drp1^{S637A}, and Drp1^{S637D} in WT 293T cells. 293T cells were co-transfected with empty vector, Myc-Drp1^{WT}, Myc-Drp1^{S637A} or Myc-Drp1^{S637D}, and MIEF1-V5, MIEF2-V5, or FLAG-Mff as indicated. Cell lysates were used for co-IP with anti-Myc beads followed by immunoblotting with indicated antibodies. The ratio between indicated proteins was analyzed by densitometry.

and Drp1^{S616D} mutants were generated from untagged WT Drp1 using the QuikChange Lightning Multi Site-Directed Mutagenesis Kit (Invitrogen).

RNA interference for gene silencing

Lipofectamine® RNAiMax (Invitrogen) was used for RNAi according to the manufacturer's protocol. Briefly, cells were seeded on 6-well plates for 16 h and transfected with siRNA; after 24 h the same siRNA was transfected and incubated for another 48 h and cells were collected for further work. Specific siRNAs used in this study were as follows: MIEF1-siRNA: 5′-GCCAAGCAAGCUGCUGUGGACAUAU-3′ (Invitrogen) and MIEF2-siRNA: 5′-CCCUGGCCGUGAAGCGGUUCAUUGA-3′ (Invitrogen); Drp1-siRNA: 5′-CCUGCUUUAUUUGUGCCUGAGG-

Figure 6. The effect of forskolin plus FK506 treatment on the Drp1 phosphorylation status of Drp1$^{-/-}$ 293T cells overexpressing untagged Drp1^{WT}, Drp1^{S637A}, and Drp1^{S637D}. *A*, subcellular localization of total Drp1 and Drp1^{pS637} as well as morphology of mitochondria in Drp1$^{-/-}$ 293T cells overexpressing untagged Drp1^{WT}, Drp1^{S637A}, and Drp1^{S637D} following forskolin plus FK506 treatment. Drp1$^{-/-}$ 293T cells were transfected with empty vector, Drp1^{WT}, Drp1^{S637A}, and Drp1^{S637D} as indicated, followed by treatment with forskolin (30 μM) plus FK506 (10 μM) for 3 h, and stained with MitoTracker (*red*), anti–phospho-Drp1(Ser-637) (*green*), and anti-Drp1(*yellow*). The high magnification views of the *boxed areas* are shown in the respective *lower panels*. *B*, 3D surface rendering reconstruction of the Drp1$^{-/-}$ 293T cells overexpressing untagged Drp1^{WT} treated with forskolin plus FK506 as shown in (*A*). Drp1^{pS637} (*green*) and mitochondria (*red*) are indicated. *Inset* represents high magnification view of the *boxed area*, in which Drp1^{pS637} localized on the mitochondrial surface is indicated by *arrows*. *C*, quantitative co-localization of mitochondria with reconstituted untagged Drp1^{WT}, Drp1^{S637A}, and Drp1^{S637D} in Drp1$^{-/-}$ cells shown in (*A*) was analyzed using the PCC (mean ± S.E.M.). *n* represents the number of cells analyzed for each condition. *D*, percentages (mean ± S.E.M.) of cells with indicated mitochondrial morphologies in Drp1$^{-/-}$ 293T cells overexpressing untagged Drp1^{WT} treated with DMSO, or Drp1$^{-/-}$ 293T cells transfected with empty vector, untagged Drp1^{WT}, Drp1^{S637A}, or Drp1^{S637D}, followed by treatment with forskolin plus FK506 as indicated in (*A*). *n* represents the number of cells analyzed. *E*, Western blot analysis showing that forskolin/FK506 treatment induces phosphorylation of Drp1^{WT}, but not of the mutants Drp1^{S637A} and Drp1^{S637D}. 293T cells treated with DMSO or forskolin/FK506 were used as controls, and Drp1$^{-/-}$ 293T cells transfected with empty vector, Drp1^{WT}, Drp1^{S637A}, or Drp1^{S637D}, followed by treatment with forskolin (30 μM) plus FK506 (10 μM) for 3 h. Cell lysates were subjected to immunoblotting with indicated antibodies. GAPDH was used as loading control.

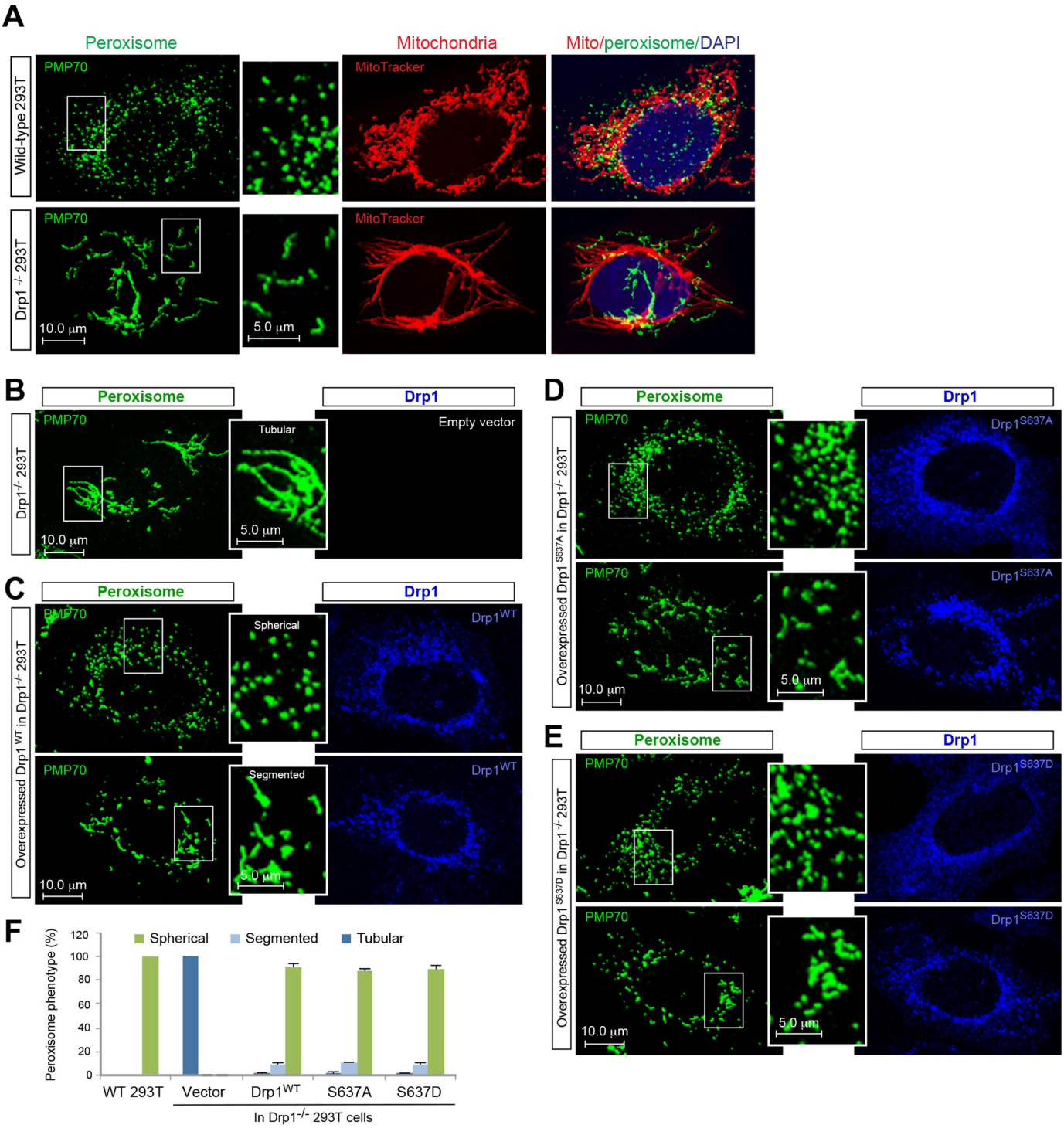

Figure 8. The phosphorylation status of Drp1 is not crucial for regulating Drp1-mediated peroxisomal fission. *A*, confocal images of mitochondria (*red*) and peroxisomes (*green*) in WT and Drp1$^{-/-}$ 293T cells. *B–E*, peroxisomal phenotypes (*green*) in Drp1$^{-/-}$ 293T cells transfected with empty vector (*B*), untagged Drp1^{WT} (*C*), Drp1^{S637A} (*D*), and Drp1^{S637D} (*E*) as indicated. *F*, percentages (mean ± S.E.M.) of cells with indicated peroxisomal phenotypes in WT 293T cells (n = 211), Drp1$^{-/-}$ cells transfected with empty vector (n = 150), and Drp1$^{-/-}$ cells reconstituted with untagged Drp1^{WT} (n = 237), Drp1^{S637A} (n = 182), and Drp1^{S637D} (n = 222), where n represents the number of cells analyzed.

UUU-3′ (Invitrogen); PKA-siRNA1 5′-CAAGGACAACUC-AAACUUAtt-3′ and PKA-siRNA2 5′-CAAGGACAACU-CAAACUUAtt-3′ (Ambion). The scrambled Stealth RNAi™ siRNA Negative Control Kit (12935-100) with similar GC content (Invitrogen) was transfected as control.

Western blotting

Protein extracts were separated by electrophoresis using NuPAGE® Novex Bis-Tris Gel (Invitrogen) and transferred to PVDF membranes with Transfer Pack (Bio-Rad). After blocking with 10% nonfat dry milk in PBS, membranes were incu-

bated with primary antibodies followed by the peroxidase-conjugated secondary antibody (GE Healthcare), and immunocomplexes were detected with the Pierce ECL Western Blotting Substrate (Thermo Fisher Scientific). Intensity of the bands on Western blots was measured using ImageJ.

Co-immunoprecipitation

Co-IP experiments were carried out as described (24, 26, 70). Briefly, cultured 293T cells were washed with PBS buffer, proteins were *in vivo* crosslinked by 1% formaldehyde in PBS buffer and the cells were scraped off with a rubber scraper and suspended in lysis buffer (PBS containing 1% Nonidet P-40 and protease inhibitor mixture cOmplete EDTA-free) (Roche Diagnostics). The cell suspensions were sonicated and centrifuged to remove insoluble debris. For the co-IP of exogenous proteins, the resulting supernatants were incubated with anti-V5 agarose or anti-Myc agarose (Novus Biologicals). For the co-IP of endogenous proteins, 2 μg of the specific antibody was incubated with Dynabeads® protein G for 1 h. After washing with lysis buffer twice, the antibody-conjugated beads were added to the resulting supernatants. Thereafter the beads were washed with PBS containing 1% Nonidet P-40 followed by PBS. The immunocomplexes captured on the agarose beads conjugated with antibody were dissolved in SDS-sample buffer and subjected to immunoblotting.

Immunofluorescence confocal microscopy and 3D surface rendering reconstruction

Immunofluorescence confocal microscopy was carried out as described (24, 26). For mitochondrial staining, the Mito-Tracker Red CMXRos (500 nM, Molecular Probes) was added to culture for 15 min before fixation. Specimens immunostained with different antibodies were examined by SP5 confocal microscopy system (Leica). Quantitative co-localization analysis of confocal images was performed with the Pearson's correlation coefficient (r) using the Leica integrated program or ImageJ, and statistical significance was determined using Student's t test. The Pearson's correlation coefficient was expressed as mean ± S.E. These experiments were performed by different persons during slide preparation and microscopy to avoid any introduction of bias. A minimum of three biological repeats was performed for all of the experiments.

The confocal images were deconvolved and 3D surface rendering was performed by the Huygens imaging software (Scientific Volume Imaging B.V.). The background estimation and signal-to-noise ratio were set automatically during deconvolution.

Subcellular fractionation

Subcellular fractionation of 293T cells was carried out as described (24, 71). Briefly, cells were harvested and homogenized in mitochondrial buffer (210 mM mannitol, 70 mM sucrose, 10 mM HEPES, 1 mM EDTA, pH 8.0 and protease inhibitor mixture cOmplete EDTA-free, Roche Diagnostics) on ice, then centrifuged 1500 × g for 5 min at 4 °C. The resulting supernatant (whole cell lysate) was pooled to a new tube and centrifuged for 30 min at 16,000 × g at 4 °C. Next, the supernatant (cytosolic fraction) was carefully separated from the pellet (mitochondrial fraction). The pellet was washed with mitochondrial buffer, and centrifuged at 16,000 × g for 15 min again. The whole cell lysate, cytosolic fraction, and mitochondrial fraction were dissolved in SDS-sample buffer and subjected to immunoblotting.

Statistical analysis

The unpaired Student's t test (http://www.physics.csbsju.edu/stats/t-test_bulk_form.html)[6] was applied to evaluate differences between experimental groups. p values less than or equal to 0.05 indicated statistical significance.

Author contributions—R. Y. and J. Z. conceptualization; R. Y. and T. L. resources; R. Y., T. L., C. N., F. T., S.-B. J., U. L., and J. Z. data curation; R. Y., T. L., C. N., F. T., U. L., and J. Z. formal analysis; U. L., J. Z., and M. N. supervision; U. L., J. Z., and M. N. funding acquisition; R. Y. and J. Z. validation; R. Y., T. L., C. N., F. T., S.-B. J., U. L., J. Z., and M. N. investigation; R. Y., T. L., C. N., F. T., S.-B. J., U. L., and J. Z. methodology; R. Y., T. L., C. N., U. L., J. Z., and M. N. writing-original draft; R. Y., U. L., J. Z., and M. N. writing-review and editing; R. Y. and J. Z. software; M. N., J. Z. and U. L. project administration.

References

1. Westermann, B. (2010) Mitochondrial fusion and fission in cell life and death. *Nat. Rev. Mol. Cell Biol.* **11,** 872–884 CrossRef Medline
2. Zhao, J., Lendahl, U., and Nistér, M. (2013) Regulation of mitochondrial dynamics: Convergences and divergences between yeast and vertebrates. *Cell. Mol. Life Sci.* **70,** 951–976 CrossRef Medline
3. Kiefel, B. R., Gilson, P. R., and Beech, P. L. (2006) Cell biology of mitochondrial dynamics. *Int. Rev. Cytol.* **254,** 151–213 CrossRef Medline
4. Okamoto, K., and Shaw, J. M. (2005) Mitochondrial morphology and dynamics in yeast and multicellular eukaryotes. *Annu. Rev. Genet.* **39,** 503–536 CrossRef Medline
5. Chan, D. C. (2012) Fusion and fission: Interlinked processes critical for mitochondrial health. *Annu. Rev. Genet.* **46,** 265–287 CrossRef Medline
6. Otera, H., and Mihara, K. (2012) Mitochondrial dynamics: Functional link with apoptosis. *Int. J. Cell Biol.* **2012,** 821676 CrossRef Medline
7. Liesa, M., Palacín, M., and Zorzano, A. (2009) Mitochondrial dynamics in mammalian health and disease. *Physiol. Rev.* **89,** 799–845 CrossRef Medline
8. Yoon, Y., Galloway, C. A., Jhun, B. S., and Yu, T. (2011) Mitochondrial dynamics in diabetes. *Antioxid. Redox Signal.* **14,** 439–457 CrossRef Medline
9. Romanello, V., Guadagnin, E., Gomes, L., Roder, I., Sandri, C., Petersen, Y., Milan, G., Masiero, E., Del Piccolo, P., Foretz, M., Scorrano, L., Rudolf, R., and Sandri, M. (2010) Mitochondrial fission and remodelling contributes to muscle atrophy. *EMBO J.* **29,** 1774–1785 CrossRef Medline
10. Ong, S. B., and Hausenloy, D. J. (2010) Mitochondrial morphology and cardiovascular disease. *Cardiovasc. Res.* **88,** 16–29 CrossRef Medline
11. Vyas, S., Zaganjor, E., and Haigis, M. C. (2016) Mitochondria and cancer. *Cell* **166,** 555–566 CrossRef Medline
12. Senft, D., and Ronai, Z. A. (2016) Regulators of mitochondrial dynamics in cancer. *Curr. Opin. Cell Biol.* **39,** 43–52 CrossRef Medline
13. Schrepfer, E., and Scorrano, L. (2016) Mitofusins, from mitochondria to metabolism. *Mol. Cell* **61,** 683–694 CrossRef Medline
14. Tilokani, L., Nagashima, S., Paupe, V., and Prudent, J. (2018) Mitochondrial dynamics: Overview of molecular mechanisms. *Essays Biochem.* **62,** 341–360 CrossRef Medline

[6] Please note that the JBC is not responsible for the long-term archiving and maintenance of this site or any other third party hosted site.

15. Panchal, K., and Tiwari, A. K. (2019) Mitochondrial dynamics, a key executioner in neurodegenerative diseases. *Mitochondrion* **47,** 151–173 CrossRef Medline
16. Filadi, R., Pendin, D., and Pizzo, P. (2018) Mitofusin 2: From functions to disease. *Cell Death Dis.* **9,** 330 CrossRef Medline
17. Rojo, M., Legros, F., Chateau, D., and Lombès, A. (2002) Membrane topology and mitochondrial targeting of mitofusins, ubiquitous mammalian homologs of the transmembrane GTPase Fzo. *J. Cell Sci.* **115,** 1663–1674 Medline
18. Chen, H., Detmer, S. A., Ewald, A. J., Griffin, E. E., Fraser, S. E., and Chan, D. C. (2003) Mitofusins Mfn1 and Mfn2 coordinately regulate mitochondrial fusion and are essential for embryonic development. *J. Cell Biol.* **160,** 189–200 CrossRef Medline
19. Pagliuso, A., Cossart, P., and Stavru, F. (2018) The ever-growing complexity of the mitochondrial fission machinery. *Cell. Mol. Life Sci.* **75,** 355–374 CrossRef Medline
20. Smirnova, E., Griparic, L., Shurland, D. L., and van der Bliek, A. M. (2001) Dynamin-related protein Drp1 is required for mitochondrial division in mammalian cells. *Mol. Biol. Cell* **12,** 2245–2256 CrossRef Medline
21. Pitts, K. R., Yoon, Y., Krueger, E. W., and McNiven, M. A. (1999) The dynamin-like protein DLP1 is essential for normal distribution and morphology of the endoplasmic reticulum and mitochondria in mammalian cells. *Mol. Biol. Cell* **10,** 4403–4417 CrossRef Medline
22. Otera, H., Wang, C., Cleland, M. M., Setoguchi, K., Yokota, S., Youle, R. J., and Mihara, K. (2010) Mff is an essential factor for mitochondrial recruitment of Drp1 during mitochondrial fission in mammalian cells. *J. Cell Biol.* **191,** 1141–1158 CrossRef Medline
23. Losón, O. C., Song, Z., Chen, H., and Chan, D. C. (2013) Fis1, Mff, MiD49, and MiD51 mediate Drp1 recruitment in mitochondrial fission. *Mol. Biol. Cell* **24,** 659–667 CrossRef Medline
24. Zhao, J., Liu, T., Jin, S., Wang, X., Qu, M., Uhlén, P., Tomilin, N., Shupliakov, O., Lendahl, U., and Nistér, M. (2011) Human MIEF1 recruits Drp1 to mitochondrial outer membranes and promotes mitochondrial fusion rather than fission. *EMBO J.* **30,** 2762–2778 CrossRef Medline
25. Palmer, C. S., Osellame, L. D., Laine, D., Koutsopoulos, O. S., Frazier, A. E., and Ryan, M. T. (2011) MiD49 and MiD51, new components of the mitochondrial fission machinery. *EMBO Rep.* **12,** 565–573 CrossRef Medline
26. Liu, T., Yu, R., Jin, S. B., Han, L., Lendahl, U., Zhao, J., and Nistér, M. (2013) The mitochondrial elongation factors MIEF1 and MIEF2 exert partially distinct functions in mitochondrial dynamics. *Exp. Cell Res.* **319,** 2893–2904 CrossRef Medline
27. Koirala, S., Guo, Q., Kalia, R., Bui, H. T., Eckert, D. M., Frost, A., and Shaw, J. M. (2013) Interchangeable adaptors regulate mitochondrial dynamin assembly for membrane scission. *Proc. Natl. Acad. Sci. U.S.A.* **110,** E1342–E1351 CrossRef Medline
28. Gandre-Babbe, S., and van der Bliek, A. M. (2008) The novel tail-anchored membrane protein Mff controls mitochondrial and peroxisomal fission in mammalian cells. *Mol. Biol. Cell* **19,** 2402–2412 CrossRef Medline
29. Yoon, Y., Krueger, E. W., Oswald, B. J., and McNiven, M. A. (2003) The mitochondrial protein hFis1 regulates mitochondrial fission in mammalian cells through an interaction with the dynamin-like protein DLP1. *Mol. Cell. Biol.* **23,** 5409–5420 CrossRef Medline
30. Yu, R., Liu, T., Jin, S. B., Ning, C., Lendahl, U., Nistér, M., and Zhao, J. (2017) MIEF1/2 function as adaptors to recruit Drp1 to mitochondria and regulate the association of Drp1 with Mff. *Sci. Rep.* **7,** 880 CrossRef Medline
31. Otera, H., Ishihara, N., and Mihara, K. (2013) New insights into the function and regulation of mitochondrial fission. *Biochim. Biophys. Acta* **1833,** 1256–1268 CrossRef Medline
32. Friedman, J. R., and Nunnari, J. (2014) Mitochondrial form and function. *Nature* **505,** 335–343 CrossRef Medline
33. Mishra, P., and Chan, D. C. (2016) Metabolic regulation of mitochondrial dynamics. *J. Cell Biol.* **212,** 379–387 CrossRef Medline
34. Prudent, J., and McBride, H. M. (2016) Mitochondrial dynamics: ER actin tightens the Drp1 noose. *Curr. Biol.* **26,** R207–R209 CrossRef Medline
35. Kraus, F., and Ryan, M. T. (2017) The constriction and scission machineries involved in mitochondrial fission. *J. Cell Sci.* **130,** 2953–2960 CrossRef Medline
36. Korobova, F., Ramabhadran, V., and Higgs, H. N. (2013) An actin-dependent step in mitochondrial fission mediated by the ER-associated formin INF2. *Science* **339,** 464–467 CrossRef Medline
37. Friedman, J. R., Lackner, L. L., West, M., DiBenedetto, J. R., Nunnari, J., and Voeltz, G. K. (2011) ER tubules mark sites of mitochondrial division. *Science* **334,** 358–362 CrossRef Medline
38. Lee, J. E., Westrate, L. M., Wu, H., Page, C., and Voeltz, G. K. (2016) Multiple dynamin family members collaborate to drive mitochondrial division. *Nature* **540,** 139–143 CrossRef Medline
39. Santel, A., and Frank, S. (2008) Shaping mitochondria: The complex post-translational regulation of the mitochondrial fission protein DRP1. *IUBMB Life* **60,** 448–455 CrossRef Medline
40. Chang, C. R., and Blackstone, C. (2010) Dynamic regulation of mitochondrial fission through modification of the dynamin-related protein Drp1. *Ann. N.Y. Acad. Sci.* **1201,** 34–39 CrossRef Medline
41. Wilson, T. J., Slupe, A. M., and Strack, S. (2013) Cell signaling and mitochondrial dynamics: Implications for neuronal function and neurodegenerative disease. *Neurobiol. Dis.* **51,** 13–26 CrossRef Medline
42. Willems, P. H., Rossignol, R., Dieteren, C. E., Murphy, M. P., and Koopman, W. J. (2015) Redox homeostasis and mitochondrial dynamics. *Cell Metab.* **22,** 207–218 CrossRef Medline
43. Taguchi, N., Ishihara, N., Jofuku, A., Oka, T., and Mihara, K. (2007) Mitotic phosphorylation of dynamin-related GTPase Drp1 participates in mitochondrial fission. *J. Biol. Chem.* **282,** 11521–11529 CrossRef Medline
44. Chang, C. R., and Blackstone, C. (2007) Cyclic AMP-dependent protein kinase phosphorylation of Drp1 regulates its GTPase activity and mitochondrial morphology. *J. Biol. Chem.* **282,** 21583–21587 CrossRef Medline
45. Cribbs, J. T., and Strack, S. (2007) Reversible phosphorylation of Drp1 by cyclic AMP-dependent protein kinase and calcineurin regulates mitochondrial fission and cell death. *EMBO Rep.* **8,** 939–944 CrossRef Medline
46. Cereghetti, G. M., Stangherlin, A., Martins de Brito, O., Chang, C. R., Blackstone, C., Bernardi, P., and Scorrano, L. (2008) Dephosphorylation by calcineurin regulates translocation of Drp1 to mitochondria. *Proc. Natl. Acad. Sci. U.S.A.* **105,** 15803–15808 CrossRef Medline
47. Merrill, R. A., Dagda, R. K., Dickey, A. S., Cribbs, J. T., Green, S. H., Usachev, Y. M., and Strack, S. (2011) Mechanism of neuroprotective mitochondrial remodeling by PKA/AKAP1. *PLoS Biol.* **9,** e1000612 CrossRef Medline
48. Shin, H. W., Takatsu, H., Mukai, H., Munekata, E., Murakami, K., and Nakayama, K. (1999) Intermolecular and interdomain interactions of a dynamin-related GTP-binding protein, Dnm1p/Vps1p-like protein. *J. Biol. Chem.* **274,** 2780–2785 CrossRef Medline
49. Zhu, P. P., Patterson, A., Stadler, J., Seeburg, D. P., Sheng, M., and Blackstone, C. (2004) Intra- and intermolecular domain interactions of the C-terminal GTPase effector domain of the multimeric dynamin-like GTPase Drp1. *J. Biol. Chem.* **279,** 35967–35974 CrossRef Medline
50. Ugarte-Uribe, B., Müller, H. M., Otsuki, M., Nickel, W., and García-Sáez, A. J. (2014) Dynamin-related protein 1 (Drp1) promotes structural intermediates of membrane division. *J. Biol. Chem.* **289,** 30645–30656 CrossRef Medline
51. Macdonald, P. J., Stepanyants, N., Mehrotra, N., Mears, J. A., Qi, X., Sesaki, H., and Ramachandran, R. (2014) A dimeric equilibrium intermediate nucleates Drp1 reassembly on mitochondrial membranes for fission. *Mol. Biol. Cell* **25,** 1905–1915 CrossRef Medline
52. Yu, R., Jin, S. B., Lendahl, U., Nister, M., and Zhao, J. (2019) Human Fis1 regulates mitochondrial dynamics through inhibition of the fusion machinery. *EMBO J.* **38,** e99748 CrossRef Medline
53. Jahani-Asl, A., Huang, E., Irrcher, I., Rashidian, J., Ishihara, N., Lagace, D. C., Slack, R. S., and Park, D. S. (2015) CDK5 phosphorylates DRP1 and drives mitochondrial defects in NMDA-induced neuronal death. *Hum. Mol. Genet.* **24,** 4573–4583 CrossRef Medline
54. Zhang, Z., Liu, L., Wu, S., and Xing, D. (2016) Drp1, Mff, Fis1, and MiD51 are coordinated to mediate mitochondrial fission during UV irradiation-induced apoptosis. *FASEB J.* **30,** 466–476 CrossRef Medline
55. Liu, R., and Chan, D. C. (2015) The mitochondrial fission receptor Mff selectively recruits oligomerized Drp1. *Mol. Biol. Cell* **26,** 4466–4477 CrossRef Medline

56. Koch, A., Thiemann, M., Grabenbauer, M., Yoon, Y., McNiven, M. A., and Schrader, M. (2003) Dynamin-like protein 1 is involved in peroxisomal fission. *J. Biol. Chem.* **278,** 8597–8605 CrossRef Medline
57. Schrader, M., Costello, J. L., Godinho, L. F., Azadi, A. S., and Islinger, M. (2016) Proliferation and fission of peroxisomes—an update. *Biochim. Biophys. Acta* **1863,** 971–983 CrossRef Medline
58. Otera, H., Miyata, N., Kuge, O., and Mihara, K. (2016) Drp1-dependent mitochondrial fission via MiD49/51 is essential for apoptotic cristae remodeling. *J. Cell Biol.* **212,** 531–544 CrossRef Medline
59. Merrill, R. A., and Strack, S. (2014) Mitochondria: A kinase anchoring protein 1, a signaling platform for mitochondrial form and function. *Int. J. Biochem. Cell Biol.* **48,** 92–96 CrossRef Medline
60. Acin-Perez, R., Salazar, E., Kamenetsky, M., Buck, J., Levin, L. R., and Manfredi, G. (2009) Cyclic AMP produced inside mitochondria regulates oxidative phosphorylation. *Cell Metab.* **9,** 265–276 CrossRef Medline
61. Lucero, M., Suarez, A. E., and Chambers, J. W. (2019) Phosphoregulation on mitochondria: Integration of cell and organelle responses. *CNS Neurosci. Ther.* **25,** 837–858 CrossRef Medline
62. Ould Amer, Y., and Hebert-Chatelain, E. (2018) Mitochondrial cAMP-PKA signaling: What do we really know? *Biochim. Biophys. Acta Bioenerg.* **1859,** 868–877 CrossRef Medline
63. Valsecchi, F., Ramos-Espiritu, L. S., Buck, J., Levin, L. R., and Manfredi, G. (2013) cAMP and mitochondria. *Physiology (Bethesda)* **28,** 199–209 CrossRef Medline
64. Kostic, M., Ludtmann, M. H., Bading, H., Hershfinkel, M., Steer, E., Chu, C. T., Abramov, A. Y., and Sekler, I. (2015) PKA phosphorylation of NCLX reverses mitochondrial calcium overload and depolarization, promoting survival of PINK1-deficient dopaminergic neurons. *Cell Rep.* **13,** 376–386 CrossRef Medline
65. Imai, Y., and Lu, B. (2011) Mitochondrial dynamics and mitophagy in Parkinson's disease: Disordered cellular power plant becomes a big deal in a major movement disorder. *Curr. Opin. Neurobiol.* **21,** 935–941 CrossRef Medline
66. Liesa, M., and Shirihai, O. S. (2013) Mitochondrial dynamics in the regulation of nutrient utilization and energy expenditure. *Cell Metab.* **17,** 491–506 CrossRef Medline
67. Autret, A., and Martin, S. J. (2009) Emerging role for members of the Bcl-2 family in mitochondrial morphogenesis. *Mol. Cell* **36,** 355–363 CrossRef Medline
68. Zhou, W., Chen, K. H., Cao, W., Zeng, J., Liao, H., Zhao, L., and Guo, X. (2010) Mutation of the protein kinase A phosphorylation site influences the anti-proliferative activity of mitofusin 2. *Atherosclerosis* **211,** 216–223 CrossRef Medline
69. Jhun, B. S., O-Uchi, J., Adaniya, S. M., Cypress, M. W., and Yoon, Y. (2018) Adrenergic regulation of Drp1-driven mitochondrial fission in cardiac physio-pathology. *Antioxidants* **7,** E195 CrossRef Medline
70. Hájek, P., Chomyn, A., and Attardi, G. (2007) Identification of a novel mitochondrial complex containing mitofusin 2 and stomatin-like protein 2. *J: Biol. Chem.* **282,** 5670–5681 CrossRef Medline
71. Zhao, J., Liu, T., Jin, S. B., Tomilin, N., Castro, J., Shupliakov, O., Lendahl, U., and Nistér, M. (2009) The novel conserved mitochondrial inner-membrane protein MTGM regulates mitochondrial morphology and cell proliferation. *J. Cell Sci.* **122,** 2252–2262 CrossRef Medline